Research Square

Preprints are preliminary reports that have not undergone peer review.
They should not be considered conclusive, used to inform clinical practice,
or referenced by the media as validated information.

Accelerating effect of Shilajit on osteogenic property of adipose derived mesenchymal stem cells (ASCs)

Parisa Kangari
Shiraz University of Medical Sciences
Leila Roshangar
Tabriz University of Medical Sciences
Aida Iraji
Shiraz University of Medical Sciences
Tahereh Talaei-Khozani
Shiraz University of Medical Sciences
Mahboobeh Razmkhah (mrazmkhah2@gmail.com)
Shiraz Institute for Cancer Research, School of Medicine, Shiraz University of Medical Sciences, Shiraz, Iran

Research Article

Keywords: Osteogenic differentiation, Shilajit, Alginate, Adipose derived mesenchymal stem cells

Posted Date: June 15th, 2022

DOI: https://doi.org/10.21203/rs.3.rs-1733994/v1

License: This work is licensed under a Creative Commons Attribution 4.0 International License.
Read Full License

Abstract

Background

Shilajit, as a herbomineral natural substance, has been most widely used remedy for treating a numerous of illness such as bone defects in Iran traditional folk medicine since hundreds of years ago. The aim of the present study was to explore the effect of Shilajit on the osteogenic differentiation of human adipose-derived mesenchymal stem cells (ASCs) in two- and three-dimensional cultures.

Materials and methods

ASCs were isolated and seeded in three-dimensional (3D) 1% alginate (Alg) hydrogel with or without Shilajit at a density of 3×10^5 cell/mL. For two-dimensional (2D) cultures, 3×10^4 ASCs /mL were seeded into culture plates and treated with 500µg/mL Shilajit. Then, characterization was done using electron microscopy (SEM)/energy dispersive X-ray spectroscopy (EDX), alkaline phosphatase (ALP) activity, Alizarin red staining, and Raman confocal microscopy.

Results

Adding Shilajit had no impact on the Alg scaffold degradability. In the 3D Alg hydrogel and in the present of osteogenic medium (OM), Shilajit acted as enhancer to increase ALP activity, also showed osteoinductive property in the absence of OM compared to the 2D matched groups at all time points (days 7 and 21 both $P < 0.001$, for 14 days $P < 0.001$ and $P < 0.05$, respectively). In addition, calcium deposition was significantly increased in the cultures exposed to Shilajit compared to 2D matched groups on days 14 ($P < 0.0001$), and 21 ($P < 0.001$and $P < 0.01$, respectively). In both 3D and 2D conditions, Shilajit induced osteogenic differentiation, but Shilajit/Alg combination starts osteogenic differentiation in a short period of time.

Conclusion

As Shilajit accelerates the differentiation of ASCs into the osteoblasts, without changing the physical properties of the Alg hydrogel, this combination may pave the way for more promising remedies considering bone defects.

Introduction

Bone defects are one of the most common mobility disabilities that cause notable health, social and economic problems. Annually, more than 20 million individuals are at risk for bone loss[1]. In the past decades, bone substitutes such as allografts, xenografts and alloplastic materials for bone defect repair have been presented, however, they may have serious limitations and side effects. In recent years, to

overcome the impediments and disadvantages associated with bone grafts, regenerative medicine approaches including cell therapy have been extensively developed[2]. Mesenchymal stem cells (MSCs) are a convenient option for cell therapy in different diseases such as bone defects. In this regard, extensive investigations has been performed on MSC therapy in bone repair alone or in combination with other remedies[3]. Systemic and local administration of allogeneic bone marrow-derived mesenchymal stem cells(BM-MSCs) in rat femoral bone fracture led to an elevation in the callus formation and osteoblast differentiation[4]. In another study, a combination of amniotic fluid-derived MSC and platelet-rich plasma (PRP) embedded in polycaprolactone scaffolds significantly improved rat cranial critical size defect, collagen type I expression and neoangiogenesis [5]. The positive impacts of MSCs on bone regeneration can be reinforced by some natural or synthetic products. For instance, in vitro studies demonstrated that curcumin [6], thymoquinone[7], polydatin[8], acemannan[9], and catalpol[10]can boost osteogenic potential of MSCs.

Shilajit, also named mineral pitch, is a herbomineral natural substance that is produced from deposition plant materials such as Euphorbia and Trifolium plants and lichen, and is one of the most widely applicable compositions with numerous therapeutic efficacies in traditional folk medicine. Shilajit is widely distributed in some parts of the world including Iran, and Altai Mountains [11], and Australia [12] with mainly same chemical compositions. It contains organic compounds (60–80%), inorganic ingredients (20–40%), and various elements[13]. Based on previous studies, the main chemical compounds of Shilajit are Fulvic acid, dibenzo-alpha-pyroons (DBPs) and DBP chromoproteins. Additionally, the overall mineral content of Shilajit are mainly composed from potassium, calcium, and magnesium, while sulfur and sodium being the next[14]. Also, Shilajit contains exogenous amino acids, such as methionine, leucine and threonine, and also endogenous amino acids such as histidine, proline, glycine, tyrosine, arginine and aspartic acid[13]. It has been revealed that Shilajit has various biological activities such as immunomodulatory, anti-inflammatory, antimicrobial, antioxidant. It also has gastroprotective, anti-cancer, spermatogenesis, oogenesis, and anti-hyperlipidemia effects[15, 16].The Shilajit antioxidant activity can be due to the presence of DBPs and fulvic acid. Besides, fulvic acid facilitates importing minerals into the target cells, protecting the electrical potential and preventing cell death [17, 18]. The safety and healing efficacy of Shilajit has been studied in humans and animals [14].The Shilajit compounds exhibits a great potential for healing the different diseases such as bone fractures, osteoarthritis[19, 20], anemia[21], diabetes[22], and Alzheimer[23]. A clinical trial conducted in Iran revealed that oral administration of Shilajit after tibia fracture surgery accelerated bone repair[24]. The findings of another cohort study in Iran indicated that Shilajit consumption had beneficial impact on femur and tibia bone fracture repair [25]. In addition, according to the results of a randomized double-blinded study, Shilajit was an effective treatment for ameliorating pain in osteoarthritis dog model due to its anti-inflammatory effects [20]. Another study showed that Shilajit is an effective treatment for chronic ulcers[26].

Although the positive effects of systematic and local administration of Shilajit on bone fracture repair was documented in traditional medicine, there are a few studies showing the effect of Shilajit on

osteogenic capacity of MSCs. In the current study, the osteogenic potential of human adipose-derived MSCs (ASCs) was compared in the presence or absence of Shilajit in both 2D and 3D culture systems.

Materials And Methods

Preparation of Shilajit

Shilajit was collected from Lorestan province altitudes, in western of Iran. 50 gr powdered Shilajit was dissolved in 500 mL distilled water. This mixture was boiled on high flame to melt, then the flame was declined until it becomes concentrated and black. Shilajit was stored at room temperature and protected from moisturizing. To prepare the appropriated concentrations, the Shilajit extract was dissolved in media or alginate(Alg) and then was sterilized through 0.22 µm syringe filter (Jet Biofil, China).

Inductively coupled plasma mass spectrometry (ICP-MS)

The mineral contents of Shilajit were analyzed by inductively coupled plasma mass spectrometry (ICP-MS). First the sample was crushed into fine powder, then 0.1 gr were treated with concentrated HNO_3 and allowed to stand for 30 minutes in room temperature. 500 µL of concentrated $HClO_4$ was added and heated at 100°C. During the heating process, 200-300 µL of concentrated hydrofluoric acid(HF) was added gradually until a clear solution was obtained. This solution was finally used for analysis via ICP spectrometer (ELAN 9000, Perkin-Elmer SCIEX).

Determination of antioxidant capacity

The 1,1-diphenyl-2-picrylhydrazyl (DPPH) method is based on the spectrophotometric measurement of DPPH° concentration at maximum absorption wavelength at 517 nm. The antioxidant molecules can quench DPPH free radicals (reduce the absorption) and convert them to a colorless or bleached product [27].

The DPPH radical-scavenging activity of Shilajit was determined according to the method of Brand-Williams with some modifications [28]. Fifty µl of various concentrations of Shilajit)10, 5,2.5,1.25, 0.625 mg/mL) (dissolved in deionized water) was added to 100 µl methanol containing 0.05 mg/mL of DPPH radical in 96 well-plate. The samples were incubated for 20 minutes at room temperature in dark, and then absorbance was measured with spectrophotometer at 517 nm wavelength.

The experiment was carried out triplicate. Radical scavenging activity was calculated using the following formula:

%Inhibition=[(Ab-Ae)/Ab] ×100

where Ab is the absorbance of the blank sample and Ae is the absorbance of Shilajit

Proton Nuclear Magnetic Resonance (H-NMR)

Shilajit sample was vortexed for about 5 minutes in D_2O at room temperature to completely dissolve and the sample was then filtered to remove any particle. The H-NMR spectra of Shilajit was recorded on a Bruker Ascend 300 spectrometer (Bruker BioSpin GmbH, Rheinstetten, Germany) equipped with a 5 mm probe. Briefly, the spectra were referenced relative to the solvent residual peak (4.7 ppm) with 1024 number of scans, 2 number of dummy scans, 1-second relaxation delay, 24670-time domain, 2.05 acquisition time, and the other parameters were set as default. Assignments of different protons were done based on the chemical shift corresponding to solvent peak (lock frequency) as well as the integrated intensity (proportional to the number of hydrogen) and coupling constant (Spin-Spin Splitting).

Cell isolation and culture

Adipose tissues were collected from the two healthy female patients aged 30 years underwent liposuction surgery and transferred to Cancer and Stem Cell Laboratory of Shiraz Institute for Cancer Research (ICR), Shiraz University of Medical Sciences. The tissues were washed with sterile 1x phosphate buffer saline (PBS) containing 1% of penicillin/streptomycin (P/S, Bioidea, Iran) to remove contaminating blood cells. Then they were cut into small pieces and incubated in 0.2% collagenase type I (Gibco, USA) for 30 minutes at 37 °C and 5% CO_2. After digestion, an equal volume of Dulbecco's modified eagle medium (DMEM, Bioidea, Iran) supplemented with 10% heat inactivated fetal bovine serum (FBS, Gibco, USA) and 1% P/S was added to the samples to neutralize the collagenase type I activity.

Then the obtained soup was centrifuged and cell pellet containing ASCs were resuspended in DMEM supplemented with 20% FBS and 1% P/S. The medium was changed every 3 days and the cells were passaged using 0.25% trypsin solution (Bioidea, Iran). ASCs from passage 3 were used for subsequent experiments.

Characterization of ASCs: Morphology and phenotype

Cell morphology was demonstrated in cell cultures from passage 3 by crystal violet staining (Acros Organics, USA). Cells were stained with 0.5% crystal violet in methanol for 10 minutes at room temperature. Excess stain was rinsed with distilled water and spindle shaped cells were observed with the microscope.

Flow cytometry was performed to analyze the surface antigen expression of isolated ASCs. Briefly, ASCs were stained with fluorescein-5-isothiocyanate (FITC)-conjugated CD45, phycoerythrin (PE)-conjugated CD34 and CD105, and peridinin–chlorophyll–protein (PerCP)-conjugated CD73 antibodies (BD, Biosciences, USA) and were incubated at 4 °C for 15 minutes in the dark. Finally, the frequency of the positive cells for each CD marker was determined using FACS Calibur flow cytometry system (BD, Biosciences, USA). Isotype antibodies were used to exclude non-specific staining of the cells and the data were analyzed by flowjo 7.6 software package (Ashland, San Diego CA, USA).

MTT assay

3-(4,5 dimethyl-2-thiazolyl)-2,5-diphenyl tetrazolium bromide) (MTT, Merck, Germany) was used to determine the appropriate and non-toxic dose of Shilajit. In short, 1×10^4 ASCs/well in 100µL DMEM containing 10% of FBS and 1% of P/S on 96-well plates were incubated with a range of concentrations of Shilajit from 5000 to 9.7 µg/ml. After 24, 48 and 72 hours, the medium was discarded, and 150 µl of 0.1% MTT solution in culture medium was added, and incubated at 37 °C for 4 hrs. Afterward, MTT was removed, and 150 µL of dimethyl sulfoxide (DMSO, Sigma-Aldrich, USA) was added and incubated at room temperature for 1h to dissolve the formazan crystal. Finally, the optical density (OD) of the formazan solution was measured with spectrophotometer at 492 nm wavelength.

Scaffold preparation

Alginate(Alg) solution was prepared from low viscosity Alg (Sigma-Aldrich, USA) dissolved in PBS 1x and stirred in a glass beaker overnight at room temperature (25°C) at a final concentration of 1% w/v. For the cell assays, obtained solution was sterile filtered using 0.22 µm syringe filter and stored at 4 °C for further usage.

Differentiation of ASCs

The osteogenic differentiation potential of ASCs was compared in different groups in the presence or absence of Shilajit in 2D and 3D cell culture.

For 3D cultures, 3×10^5 ASCs/mL were suspended in 1% (w/v) Alg with or without 500µg/ml Shilajit, and gelation was induced by adding 2.5% $CaCl_2$. The cells were cultured with or without osteogenic medium (OM, Kiazist, Iran) supplementation for 7, 14 and 21 days. The 3D cultures were divided into four groups: (1) Shilajit/Alg/ASCs+ OM, (2) Alg/ASCs+OM (positive control), (3) Shilajit/Alg/ASCs, and (4) Alg/ASCs (negative control). The cells in negative control cultures received basic medium (DMEM containing 10% FBS and 1% P/S).

For 2D cultures, 3×10^4 cells/mL were seeded in basic medium. Upon 70% confluency, a matched 2D cultures also was performed for 7, 14 and 21 days. The 2D treatments include with the cultures exposed to either OM and 500µg/ml Shilajit at a ratio of 1/2, the same concentration of Shilajit in DMEM, positive control that received OM, or negative control. The media were changed every 3 days for both 2D and 3D groups.

Mineralization assay

After 21 days of differentiation, morphological characterization of encapsulated ASCs within the hydrogels as well as calcium and phosphorus content were respectively evaluated using scanning electron microscopy (SEM) and energy dispersive X-ray spectroscopy (EDX). Briefly, hydrogels were lyophilized, samples were fractured into pieces, then, the cut off were coated by gold replica using Q150R-ES sputter coater (Quorum Technologies, London, UK) and SEM imaging were taken using a VEGA3 microscope (TESCAN, Brno, Czech Republic) at 10 kV accelerating voltage. EDX was also performed to

evaluate the amount of calcium and phosphorous within the scaffolds. For EDX, three repeats from every group were made.

To assess alkaline phosphatase (ALP) activity, total protein of the differentiated cells was extracted at 7, 14, and 21 days, and ALP colorimetric assay kit (Pars Aazmoon, Iran) was used to evaluate the ALP activity in lysates. To do this, at each point of time, the culture medium was aspirated and the cells were washed with PBS. For extraction of total protein, cells were lysed in the buffer containing 0.2% Triton X-100 in 20 mM Tris-HCl on ice for 15 minutes. For 3D cultures, the Alg scaffolds were first exposed to 55 mM sodium citrate for depolymerization at 25 °C for 25 minutes. Then, the cells were lysed by adding the same lyses buffer. The cell lysate was centrifuged at 2500 g at 4 °C for 15 minutes, and the supernatant was used to assay ALP activity. Total protein was finally used for normalizing the enzyme activity level (U).

Alizarin Red S staining was applied to evaluate the calcium deposition. After 7, 14, and 21 days of differentiation, culture medium was aspirated, the 2D and 3D cultures were washed in PBS and fixed in 10% formaldehyde for 30 minutes. Following double washes with PBS, the samples were stained with 2 % Alizarin Red S (Sigma Aldrich) for 10 minutes. Additionally, quantitative analysis of calcium content was performed by adding 500 µL of 100 mM cetylpyridinium chloride monohydrate (Merck, Germany) to elute alizarin red S. Then absorbance was evaluated at 405 nm.

Confocal Raman microscope

After 21 days of differentiation, all 3D samples were lyophilized, and fractured into pieces, then, the Raman spectra of the cell laden scaffolds along with Shilajit were obtained by Lab-Ram HR Confocal Raman spectrometer (Horiba, Japan). Both Shilajit and 3D samples were excited with laser power level at 50 mW using the excitation laser with the wavelength of 785 nm with 100 mV power for Raman spectra recording. We analyzed the Raman shift at the range of 500-2000 cm^{-1}.

Biodegradation test

The in vitro biodegradation test was carried out to evaluate the possible impact of Shilajit on the degradation rate of Alg hydrogel scaffolds. To do this, 1% Alg hydrogels were prepared in the present or absence of Shilajit and electrogellate by 2.5% $CaCl_2$ (n =3). Prior to enzyme application, the scaffolds were weighed. Then 500 µL of 0.01% trypsin (Bioidea, Iran) was added, and incubated at 37 °C for 12, 24,48, 72,100 and 122 hours. At the selected time points, trypsin was completely removed and experimental plates weighed. The enzymatic degradation rate was calculated by subtracting the start and end weight of the scaffolds.

Scratch assay (wound healing assay)

ASCs were seeded at 3×10^4 cells/well and permitted to adhere and form a confluent. A scratch as a straight line through the center of each well was formed by a sterile 10 µl pipette tip and the wells were

washed with PBS to remove cell debris. After that, 500µL of DMEM with or without Shilajit was added to each well as treated and untreated groups. The staining was done with crystal violet at zero, 8 and 12 hours after incubation. The cell migration to the scratch was evaluated in both treated and untreated groups using the Image j software(https://imagej.nih.gov/ij/index.html). The cell free area in each group was calculated at each point of time.

Statistical analysis

Graph Pad Prism software version 8.1 was used to analysis and depicted the graphs. One-way ANOVA and two-way ANOVA were applied for compare the data from multiple groups. The results were displayed as mean ± standard error mean (SEM)and p value < 0.05 was defined as significant. All experiments were performed in triplicate.

Results

Inorganic composition of Shilajit

ICP-MS showed the presence of the high level of calcium(Ca), aluminum(Al), potassium(k), magnesium(Mg) and sodium(Na) (all 100ppm). A lower amount of the other elements such as sulfur(S), phosphorus (P)and manganese (Mn) (50, 10 and 5 ppm, respectively) was found in Shilajit. As Table 1 indicates, the amount of the other minerals was the least.

Table 1. Elemental composition of Shilajit.

Elements	Concentration of Element (ppm)
Al	100
Ca	100
Fe	100
K	100
Na	100
S	50
P	10
Ti	10
Zr	5
Mn	5
Ba	1
Co	1
Cr	1
Cu	1
Li	1
Zn	1
La	1

Antioxidant activity

The antioxidant activity of Shilajit was calculated as the percentage scavenging activity against DPPH radical. Shilajit showed 49.84 ± 1.96 % and 30.07 ± 0.24 % of DPPH inhibition at 5 and 2.5 mg/mL, respectively. The results indicated that Shilajit inhibited free radicals at the tested concentrations.

H-NMR spectrum

The H-NMR spectra of the Shilajit is depicted in Figure 1. To better analyze the H-NMR results, the spectra is divided into four main regions. The first region, from 0 to 1.8 ppm, is generally assigned to protons on methyl and methylene carbons directly bonded to other carbons. The second region, from 1.8 to 3.0 ppm, can be assigned to protons on methyl, methylene, and methane carbons which are bonded to electronegative functional groups such as aromatic rings, or carbonyls moieties. The third one is chemical shift from 3.0-4.5 that belongs to the polysaccharide. The fourth region (6.0 to 8.0 ppm) is assigned to the presence of both aromatic and heteroaromatic protons with the contribution of the unsaturated groups [29-31].

Phenotype and morphological identification of ASCs

Phenotypic characterization of cultured ASCs at passage 3 was assessed using flow cytometry. The results demonstrated that the cells expressed mesenchymal markers such as CD73 and CD105, while they were negative for hematopoietic markers such as CD34 and CD45 (Figure 2A). Additionally, the crystal violet staining of ASCs was performed and microscopic observations with light inverted microscope validated their spindle and fibroblast-like morphology (Figure 2B).

Cytotoxicity assessment

To obtain the appropriate dose of Shilajit, the survival rate of ASCs in the presence of different concentrations (9.7-5000 µg/mL) of Shilajit was evaluated. As MTT test showed supplementation of 500 µg/mL of Shilajit had no cytotoxic effect, and so, this concentration was used for in vitro investigations.

Mineralization assessments

SEM images revealed the round, osteoblast-like cells with few filopodia for the cells encapsulated in Shilajit/Alg with or without OM ,and Alg/ASCs+OM. However, in the absence of both Shilajit and OM, the cells were spindle and fibroblast like shape, the typical phenotype of MSCs (Figure 3).

According to the results from EDX analyses, the highest level of calcium and phosphorus deposition was observed in the Shilajit/Alg/ASCs+OM ($P<0.001$ and $P<0.01$ for Alg/ASCs+OM, respectively), (both $P<0.0001$ for Shilajit/Alg/ASCs and Alg/ASCs). In addition, Alg/ASCs+OM presented a significant increase in the level of calcium and phosphorous deposition compared to both Shilajit/Alg/ASCs (for both $P<0.01$) and Alg/ASCs (for both $P<0.0001$). However, the amount of calcium and phosphorous was higher in the Shilajit/Alg/ASCs than Alg/ASCs ($P<0.01$ and $P<0.001$, respectively) (Figure 4A, B).

The ALP activity was estimated in the various experimental groups on days 7, 14 and 21. ALP activity was significantly higher in the cultures received both Shilajit and OM on 7 ($P<0.0001$), 14 and 21 days ($P<0.001$) compared with Alg/ASCs+OM that indicates the boosting impact of Shilajit on OM. Although the Shilajit had osteoinductive property in all points of time, the Shilajit was not as effective as OM in elevating ALP activity. Therefore, ALP activity displayed a significantly elevation in Shilajit/Alg/ASCs+OM compared with Shilajit/Alg/ASCs ($P<0.01$ for 7 days; $P<0.0001$ for 14 and 21 days). In addition, Shilajit/Alg/ASCs could significantly elevate the ALP activity compared to Alg/ASCs without OM ($P<0.0001$ for all time points) or with OM on day 7 ($P<0.05$), while at day 21 ALP activity increased in Alg/ASCs+OM than Shilajit/Alg/ASCs ($P<0.01$). Indeed, ALP activity increased in Alg/ASCs+OM compared with Alg/ASCs ($P<0.01$ for day 7; $P<0.0001$ for days 14 and 21) (Figure 5A).

In 2D conditions, Shilajit supplementation also boosted the osteogenic effect of OM as ALP activity increased significantly in Shilajit+OM treated compared to the cultures treated with either OM ($P<0.01$, all time points) or Shilajit alone (for day 7 $P<0.05$, day 14 $P<0.01$, and day 21 $P<0.0001$) and untreated control (for 7days$P<0.01$, for 14 and 21 days $P<0.0001$). On days 14 and 21, Shilajit also caused a significant increase in ALP activity even in the absence of OM compared to the negative control cultures ($P<0.05$; Figure 5B).

Comparing 3D and 2D cultures displayed that ALP activity was significantly higher in 3D culture conditions than matched groups of 2D conditions except for negative matched groups. The ALP activity of the cells encapsulated in Shilajit/Alg/ASCs+OM, and Shilajit/Alg/ASCs was higher compared to the 2D matched groups at all time points (days 7 and 21 both $P<0.001$, for 14 days $P<0.001$ and $P<0.05$, respectively). In addition, Alg/ASCs+OM for 14 and 21 days exhibited significant higher ALP activity than2D condition ($P<0.01$). As the time progress, the 3D and 2D cultures in presence both Shilajit and OM showed a significant enhancement in ALP activity on day 14 compared to the same groups on days 7($P<0.01$) and 21 as well as the same groups on days 7 and 14($P<0.0001$ and $P<0.01$, respectively; Figure 5C).

Alizarin Red S staining was performed to evaluate calcium deposition. The results indicated that the highest calcium was deposited in Shilajit/Alg/ASCs+OM at each time point. In 3D conditions, the accumulation of calcium significantly increased in the Shilajit/Alg/ASCs+OM compared to Alg/ASCs+OM, Shilajit/Alg/ASCs($P<0.01$), and Alg/ASCs($P<0.001$) on day 7. The same trend was also found on days 14 and 21; so that, the cells in 3D cultures and in the presence of both Shilajit and OM deposited significantly more calcium compared the cultures deprived either Shilajit ($P<0.01$ for both 14 and 21 days) or OM ($P<0.05$ and $P<0.0001$ for 14 and 21 days, respectively). Besides, on 14 and 21 days, the least calcium deposition belong to the negative control ($P<0.0001$, Figure 5D).

In the same way with 3D conditions, in the 2D conditions, exposure the cells with a combination of OM and Shilajit resulted a significantly higher level of calcium deposition compared to their counterpart deprived either Shilajit or OM (for 14 days $P<0.01$ and $P<0.0001$, respectively; for 21 days $P<0.01$ and $P<0.0001$, respectively). Beside, adding either Shilajit or OM alone also boosted the mineralization compared to negative control at day14 (both $P<0.001$) and 21(both $P<0.0001$). In addition, an obvious increasing in mineralization was done by ASCs cultured in OM compared to the cells exposed Shilajit 21 day ($P<0.01$, Figure 5E).

3D conditions provided a superior environment for calcium deposition, so that calcium content was significantly higher in both Shilajit containing cultures and Alg/ASCs+OM compared to the matched 2D cultures on days 14 ($P<0.0001$), and 21 ($P<0.001$, $P<0.01$, and $P<0.001$, respectively), however, on day 7, Shilajit could just increase the calcium deposition in 3D cultures at the presence of OM, therefore, the higher calcium content was found in the Shilajit/Alg/ASCs+OM compared to matched 2D cultures treated with Shilajit and OM ($P<0.001$). The calcium deposition also significantly increased in 3D and 2D cultures in all groups as the time progress, so, more calcium was deposited on day 21 compared to the same groups on day 7 ($P<0.0001$). Similarly, enhancement of calcium deposition was observed in 3D and 2D cultures in the presence of both Shilajit and OM or only OM on day 21 compared to the same groups on day 14 ($P<0.001$, and $P<0.0001$, respectively, Figure 5F).

The microscopic images also confirmed that the calcium deposition was not started massively on day 7 and, the calcium amount was similar in all samples. On day 14 and 21, the most intense staining was observed in the cultures supplemented with OM, Shilajit, or the combination of both with the highest

intense staining in the last one. At 21 days, nodule size of calcium displayed a notable increment in all Shilajit compared to the similar cultures on day 14 (Figure 5G).

Confocal Raman microscope

In order to determine the contents of matrix, confocal Raman spectroscopy was randomly executed in four various regions of scaffolds on day 21 after osteogenic induction in 3D groups (Figure 6A).The Raman peaks corresponding to the different compositions related to the osteogenic differentiation process consisting cholesterol and cholesterol ester at 702 cm^{-1},protein band and proteins such as collagen type I at 820cm^{-1}, hydroxyapatite at 966 cm^{-1}, phenylalanine at 1000cm^{-1},carbonate symmetric stretching vibration of calcium carbonate apatite at 1073cm^{-1}.The peaks for carbohydrate were assigned at 1105 cm^{-1}. C-C (&C-N) stretching of proteins (also carotenoids) at1155cm^{-1}, carbon particle at 1350cm^{-1}, and deoxyribose at 1424cm^{-1} were also detected[32]. The results indicated that peak intensity is significantly higher in the Shilajit/Alg/ASCs+OM cultures. The trend of Raman spectra in the Shilajit/Alg/ASCs+OM, Shilajit/Alg/ASC and Alg/ASC+OM was the same.

In addition, confocal Raman spectroscopy was carried out to determine the molecular content of Shilajit (Figure 6B). A peak at 702 cm^{-1}represents cholesterol and cholesterol ester. Peak at 815cm^{-1}represents proline, hydroxyproline, tyrosine, and v_2 PO^-_2 stretch of nucleic acid. Peak at 865$cm^{-1}$is related to C-C stretching, hypro (collagen assignment), monosaccharides (β-fructose), (C-O-C) skeletal mode, disaccharide (sucrose), (C-O-C) skeletal mode polysaccharides, amylose polysaccharides, and amylopectin. The Raman spectrum also revealed some peaks corresponding to the different compositions including phenylalanine at 1000 cm^{-1},carbohydrates at 1105 cm^{-1}, v(C-N), proteins (protein assignment) v(C-C), carotenoid due to C-C and conjugated C55Cband stretch at 1152cm^{-1},C-C_6H_5 stretch mode (one of C-C ring vibration to be expected in aromatic structure of xylene) at 1203 cm^{-1}, amide III, adenine, and cytosine at 1258 cm^{-1}[32].

Scratch wound healing assay (SWH) &

The effect of Shilajit on ASC proliferation/movement capability was appraised quantitatively by determining healing/wounded area ratio, imitating the wound healing process. Although cell proliferation/movement happens after 8 and 12 hours in both treated and untreated groups compared to the beginning of the test (Figure 7A), a significant elevation of healing was observed in the area of the scratched site of Shilajit treated group compared to untreated group ($P<0.01$ for both) (Figure 7B).

Biodegradation

The rate of biodegradation of the scaffolds was statistically equal regardless of the presence or absence of Shilajit. After 122 hours, both scaffolds were completely degraded. Therefore, Shilajit had no adverse effect on scaffold degradation (Figure 8).

Discussion

Exceeding inflammation and calcium content depletion following bone fracture can lead to elevated the chance of damage and lagging bone healing period[25, 33]. One of the main goals of remedy prescription is to achieve bone healing in the shortest time frame using different methods such as therapy with various stem cells without or in combination with a variety of scaffolds such as hydrogels [34]. Among the hydrogels, alginate supports osteogenic differentiation, acts as an exogenous extracellular matrix and is tempting for tissue engineering due to its favorable properties, including biocompatibility, cytocompatibility, and biodegradability, and ease of gelation[35]. Besides, combining this system with traditional medicine would lead to more outstanding outcomes in regeneration of bone defects.

Here, for the first time, we show that Shilajit in 3D condition, promote osteoblast differentiation of Alg encapsulated ASCs compared to 2D cultures with or without OM. Shilajit not only showed osteoinductive properties but boosted the osteogenic impact of OM. These findings are in line with what has been indicated for Shilajit in previous studies. Based on in vitro evidence, Shilajit can prevent osteoclastogenesis, while induces osteoblastic differentiation of MSCs and boost mineralization [31, 36]. Systemic administration of Shilajit to patients with tibial and femoral fracture accelerated bone formation compared to placebo groups[24, 25]. In vivo studies in a rat osteoporotic model revealed that Shilajit may enhance bone formation rate via synthesis of polysaccharides, nucleic acids, and most proteins and hormones needed for cells and tissues growth[37]. Additionally, in line with our findings, in vitro treatment of osteoblast like cells, MG63 cells, with Shilajit enhanced osteoblast proliferation [37, 38]. Accordingly, based on the in vitro results of our study, Shilajit showed osteoinductive capability as well.

The analysis of Shilajit in the current study represented that it is an appropriate source of elements such as calcium and magnesium. Also, our findings displayed that Shilajit contains biological macromolecules including proteins and amino acids (proline, hydroxyproline, tyrosine, phenylalanine), nucleic acids and nucleotides (adenine, and cytosine), carbohydrates (monosaccharides, disaccharides, and polysaccharides), and lipids (cholesterol and cholesterol ester). Collagen as one of the most important osteogenic proteins was detected in Shilajit. There are several studies that indicate Shilajit can facilitate bone fracture healing probably because of increasing collagen synthesis, decreasing inflammation and swelling, infection control and improving oxygenation to wound area[14, 39, 40]. Interestingly, ions play prominent roles in regulating many cell functions and biological processes such as cell mitosis, osteogenesis, angiogenesis and antibacterial properties, therefore, they are great applicable in bone regeneration process [41]. Shilajit can be involved in osteogenesis through anabolic activities such as increasing synthesis of proteins and nucleic acids, and transportation of minerals into bone tissue [42]. It has also the potential to induce calcium deposition and promote bone mineralization and osteogenesis [36]. It has been reported that the abundant mineral ingredients, such as calcium and magnesium play vital roles in the process of osteogenesis. These ions via upregulating the expression of osteopontin, osteocalcin, ALP, and collagen type I, inducing osteoblast activity and increasing cell viability can influence bone formation [43–45].

Another interesting approach in regenerative medicine is controlled drug delivery. One of the major mechanisms of release of therapeutic agents in damaged tissue is using degradable materials. Biodegradable property of Alg is an advantageous approach in drug delivery and tissue engineering[46]. Natural and synthetic materials can change the degradation of Alg based scaffolds. It was displayed that an increase in Aloe Vera content enhances the degradation rate of the alginate hydrogel films[47], whereas, adding polyethylene glycol to the alginate-based microcapsules did not affect degradation rate of microcapsules[48]. Based on the results obtained from biodegradation test, Shilajit incorporation had no significant impact on physical property of Alg scaffold. Both Shilajit/Alg combination and Alg had gradually degraded during four days in the same rate and, ultimately both of them completely collapsed after 122 hrs.

Antioxidant activity is one of the major properties of Shilajit[15], which is confirmed by our data too. Compounds with antioxidant activity as direct scavengers of reactive oxygen species, can contribute to the differentiation of osteoblasts and bone formation via inhibition of NF-κB activation and also downregulation of TNF-α and RANKL expression[49]. Therefore, Shilajit can inhibit bone loss and promote bone repair due to it's antioxidant activity.

Das and coworkers) 2019) reported that oral consumption of Shilajit can affect skin health and rejuenery by stimulating endothelial cell migration and growth of blood vessels [50]. Likewise, it is showed that Shilajit has rewarding effects on wound healing process in mice model [39]. Our data displayed that Shilajit not only showed any cytotoxic effects on ASCs but also promoted cell proliferation; therefore, we checked the osteogenic induction of the highest dose of Shilajit with the most survival benefit. Also, in the current study, we carried out scratch test to investigate Shilajit effect on ASCs migration. Our data confirmed previous results and showed that Shilajit promote the healing of scratch area by triggering cell migration and proliferation, whereas treated ASCs maintained spindle-shaped morphology. The migration of endogenous and exogenous MSCs with normal morphology to sites of bone defects is a pivotal issue to start osteogenic differentiation of MSCs and skeletal development. According to researches, the ASCs migration enhancement can induce osteoblast differentiation via upregulation of expression of early growth response 1 and activation of mitogen-activated protein kinases (MAPKs)[51].

Conclusion

Altogether, Shilajit/Alg scaffold presented a great potential for promoting and accelerating ASCs' differentiation into osteocyte lineage. Accordingly, this scaffold may provide a new strategy for bone tissue engineering and can be a good therapeutic approach for the treatment of bone defects.

Abbreviations

ASCs
Human adipose derived mesenchymal stem cells
2D

Two-dimensional
3D
Three-dimensional
OM
Osteogenic medium
ALP
Alkaline phosphatase
SEM
Scanning electron microscopy
EDX
Energy dispersive X-ray spectroscopy
Alg
Alginate
MSCs
Mesenchymal stem cells
DBPs
Dibenzo-alpha-pyroons
BM-MSC
Bone marrow-derived mesenchymal stem cells
DMEM
Dulbecco's modified eagle medium
FBS
Fetal bovine serum
PBS
Phosphate-buffered saline
OD
Optical density.

Declarations

Ethics approval and consent to participate

The present study was approved by the ethics committee of Shiraz University of Medical Sciences (Ethics Committee Code No. IR.SUMS.REC.1398.506). Donors provided written and signed informed consent to have the possibility of testing on their samples.

Consent for publication

Not applicable

Availability of data and materials

All data generated or analyzed during this study are included in this published article.

Competing interests

The authors declare that they have no competing interests.

Funding

This study was financially supported by the Shiraz University of Medical Science, Shiraz, Iran (Grant No. 97-01-74-19058) and ICR (Grant No. ICR-100-504).

Authors'contributions

PK performed all the experiments and was involved in the data collection, analysis, interpretation, and manuscript drafting. LR conceived the original idea and supervised the project. MR and TTK conceived the original idea, found acquisition, supervised the project, interpreted the data and revised the manuscript. Al contribute to the composition determination of Shilajit. All authors read and approved the final manuscript.

Acknowledgements

The authors would like to thank Shiraz Institute for Cancer Research (ICR) for technical support. This research was accomplished as a commitment for the Ph.D. thesis of Applied Cell Sciences by Ms. Parisa Kangari.

Authors' information

[1]Student Research Committee, Shiraz University of Medical Sciences, Shiraz, Iran. [2]Department of Tissue Engineering and Applied Cell Sciences, School of Advanced Medical Sciences and Technologies, Shiraz University of Medical Sciences, Shiraz, Iran. [3]Shiraz Institute for Cancer Research, School of Medicine, Shiraz University of Medical Sciences, Shiraz, Iran. [4]Stem Cell Research Center, Tabriz University of Medical Sciences, Tabriz, Iran. [5]Central Research Laboratory, Shiraz University of Medical Sciences, Shiraz, Iran. [6]Stem Cell and Transgenic Technology Research Center, Shiraz University of Medical Sciences, Shiraz, Iran. [7]Tissue Engineering Laboratory, Department of Anatomy, School of Medicine, Shiraz University of Medical Sciences, Shiraz, Iran

References

1. Habibovic P. Strategic directions in osteoinduction and biomimetics. Tissue Eng Part A. 2017;23(23–24):1295–6.
2. Chaparro O, Linero I. **Regenerative medicine: a new paradigm in bone regeneration**. Advanced techniques in bone regeneration 2016(12).

3. Kangari P, Talaei-Khozani T, Razeghian-Jahromi I, Razmkhah M. Mesenchymal stem cells: amazing remedies for bone and cartilage defects. Stem Cell Res Ther. 2020;11(1):1–21.
4. Huang S, Xu L, Zhang Y, Sun Y, Li G. Systemic and local administration of allogeneic bone marrow-derived mesenchymal stem cells promotes fracture healing in rats. Cell Transplant. 2015;24(12):2643–55.
5. Ghaffarinovin Z, Soltaninia O, Mortazavi Y, Esmaeilzadeh A, Nadri S. Repair of rat cranial bone defect by using amniotic fluid-derived mesenchymal stem cells in polycaprolactone fibrous scaffolds and platelet-rich plasma. BioImpacts: BI. 2021;11(3):209 – 217.
6. Wang N, Wang F, Gao Y, Yin P, Pan C, Liu W, Zhou Z, Wang J. Curcumin protects human adipose-derived mesenchymal stem cells against oxidative stress-induced inhibition of osteogenesis. J Pharmacol Sci. 2016;132(3):192–200.
7. Rahmani-Moghadam E, Talaei-Khozani T, Zarrin V, Vojdani Z: **Thymoquinone loading into hydroxyapatite/alginate scaffolds accelerated the osteogenic differentiation of the mesenchymal stem cells**. *BioMedical Engineering OnLine* 2021, **20**(1):1–20.
8. Shen Y-S, Chen X-J, Wuri S-N, Yang F, Pang F-X, Xu L-L, He W, Wei Q-S. Polydatin improves osteogenic differentiation of human bone mesenchymal stem cells by stimulating TAZ expression via BMP2-Wnt/β-catenin signaling pathway. Stem Cell Res Ther. 2020;11(1):1–15.
9. Boonyagul S, Banlunara W, Sangvanich P, Thunyakitpisal P. Effect of acemannan, an extracted polysaccharide from Aloe vera, on BMSCs proliferation, differentiation, extracellular matrix synthesis, mineralization, and bone formation in a tooth extraction model. Odontology. 2014;102(2):310–7.
10. Zhu Y, Wang Y, Jia Y, Xu J, Chai Y. Catalpol promotes the osteogenic differentiation of bone marrow mesenchymal stem cells via the Wnt/β-catenin pathway. Stem Cell Res Ther. 2019;10(1):1–14.
11. Aiello A, Fattorusso E, Menna M, Vitalone R, Schröder HC, Müller WE: **Mumijo traditional medicine**: **fossil deposits from antarctica** (**chemical composition and beneficial bioactivity**). *Evidence-Based Complementary and Alternative Medicine* 2011, **2011**:1–8.
12. Ding R, Zhao M, Fan J, Hu X, Wang M, Zhong S, Gu R. Mechanisms of generation and exudation of Tibetan medicine Shilajit (Zhaxun). Chin Med. 2020;15(1):1–15.
13. Kloskowski T, Szeliski K, Krzeszowiak K, Fekner Z, Kazimierski Ł, Jundziłł A, Drewa T, Pokrywczyńska M. Mumio (Shilajit) as a potential chemotherapeutic for the urinary bladder cancer treatment. Sci Rep. 2021;11(1):1–12.
14. Stohs SJ, Singh K, Das A, Roy S, Sen CK. Energy and Health Benefits of Shilajit. In: Sustained Energy for Enhanced Human Functions and Activity. Elsevier; 2017. pp. 187–204.
15. Bhavsar SK, Thaker AM, Malik JK: **Shilajit**. In: *Nutraceuticals.* Elsevier; 2016: 707–716.
16. Carlos C, Leonardo G, Ricardo B. Shilajit: a natural phytocomplex with potential procognitive activity. Int J Alzheimer's Dis. 2012;10:1–4.
17. Wilson E, Rajamanickam GV, Dubey GP, Klose P, Musial F, Saha FJ, Rampp T, Michalsen A, Dobos GJ. Review on shilajit used in traditional Indian medicine. J Ethnopharmacol. 2011;136(1):1–9.

18. Sharma V, Saini DS: **Performance investigation of advanced multi-hop and single-hop energy efficient LEACH protocol with heterogeneous nodes in wireless sensor networks**. In: 2015 *Second International Conference on Advances in Computing and Communication Engineering: 2015*. IEEE: 192–197.
19. Azizi S, Kheirandiah R, Azari O, Torabi N. Potential pharmaceutic effect of Shilajit (mumie) on experimental osteoarthritis in rat. Comp Clin Pathol. 2018;27(3):755–64.
20. Lawley S, Gupta R, Goad J, Canerdy T, Kalidindi S. Anti-inflammatory and anti-arthritic efficacy and safety of purified shilajit in moderately arthritic dogs. J Vet Sci Anim Husb. 2013;1(3):1–6.
21. Velmurugan C, Vivek B, Shekar S, Sudha S, Sundaram T. Shilajit in management of iron deficiency anaemia. J Pharm Biomed Sci. 2010;1(1):1–2.
22. Winkler J, Ghosh S. Therapeutic potential of fulvic acid in chronic inflammatory diseases and diabetes. J Diabetes Res. 2018;2018:1–7.
23. Rao RV, Descamps O, John V, Bredesen DE. Ayurvedic medicinal plants for Alzheimer's disease: a review. Alzheimers Res Ther. 2012;4(3):1–9.
24. Sadeghi SMH, Hosseini Khameneh SM, Khodadoost M, Hosseini Kasnavieh SM, Kamalinejad M, Gachkar L, Rampp T, Pasalar M. Efficacy of Momiai in Tibia fracture repair: a randomized double-blinded placebo-controlled clinical trial. J Altern Complement Med. 2020;26(6):521–8.
25. Dehghan M, Faradonbeh AS. The effect of mummy on the healing of bone fractures. Afr J Pharm Pharmacol. 2012;6(5):305–9.
26. Moghadari M, Rezvanipour M, Mehrabani M, Ahmadinejad M, Tajadini H, Hashempur MH. Efficacy of mummy on healing of pressure ulcers: A randomized controlled clinical trial on hospitalized patients in intensive care unit. Electron physician. 2018;10(1):6140.
27. Ferreira IC, Baptista P, Vilas-Boas M, Barros L. Free-radical scavenging capacity and reducing power of wild edible mushrooms from northeast Portugal: Individual cap and stipe activity. Food Chem. 2007;100(4):1511–6.
28. Thaipong K, Boonprakob U, Crosby K, Cisneros-Zevallos L, Byrne DH. Comparison of ABTS, DPPH, FRAP, and ORAC assays for estimating antioxidant activity from guava fruit extracts. J Food Compos Anal. 2006;19(6–7):669–75.
29. Gigliotti G, Macchioni A, Zuccaccia C, Giusquiani P, Businelli D. A spectroscopic study of soil fulvic acid composition after six-year applications of urban waste compost. Agronomie. 2003;23(8):719–24.
30. Francioso O, Sanchez-Cortes S, Tugnoli V, Ciavatta C, Gessa C. Characterization of peat fulvic acid fractions by means of FT-IR, SERS, and 1H, 13C NMR spectroscopy. Appl Spectrosc. 1998;52(2):270–7.
31. Jung CR, Schepetkin IA, Woo SB, Khlebnikov AI, Kwon BS. Osteoblastic differentiation of mesenchymal stem cells by mumie extract. Drug Dev Res. 2002;57(3):122–33.
32. Movasaghi Z, Rehman S, Rehman IU. Raman spectroscopy of biological tissues. Appl Spectrosc Rev. 2007;42(5):493–541.

33. Mullis BH, Gudeman AS, Borrelli J Jr, Crist BD, Lee MA, Evans AR. Bone healing: Advances in biology and technology. OTA Int. 2021;4(2S):e100.
34. Gómez-Barrena E, Rosset P, Lozano D, Stanovici J, Ermthaller C, Gerbhard F. Bone fracture healing: cell therapy in delayed unions and nonunions. Bone. 2015;70:93–101.
35. Sarker B, Boccaccini AR. Alginate utilization in tissue engineering and cell therapy. In: Alginates and Their Biomedical Applications. Springer; 2018. pp. 121–55.
36. Dashnyam K, Bayaraa O, Mandakhbayar N, Park J-H, Lee J-H, Jang T-S, Luvsan K, Kim H-W. Nanoscale calcium salt-based formulations as potential therapeutics for osteoporosis. ACS Biomaterials Science & Engineering. 2020;6(8):4604–13.
37. Labban NY. Shilajit, a novel regulator of bone/cartilage healing. Indiana University; 2013.
38. Abbasi N, Azizpour Y, Azizi M, Karimi E, Aidy A, Asadollahi K. The effects of mumie extract on cell proliferation and enzyme expression of human osteoblast-like cells (MG63). J stem cells regenerative Med. 2019;15(2):18–23.
39. Rezvanipour MPF, Malekpour R, et al. The effect of mummy on some indices of wound healing in mice. J Kerman Uni Med Sci. 2007;14(4):267–77.
40. Azari Omid KRSV, Salari Amin R. Efficacy of mummy on healing of skin wound of rabbit. Sabzevar Univ Med Sci. 2011;18:158–65.
41. Perez RA, Seo S-J, Won J-E, Lee E-J, Jang J-H, Knowles JC, Kim H-W. Therapeutically relevant aspects in bone repair and regeneration. Mater Today. 2015;18(10):573–89.
42. Barouji SR, Saber A, Torbati M, Fazljou SMB, Khosroushahi AY. Health Beneficial Effects of Moomiaii in Traditional Medicine. Galen Med J. 2020;9:e1743.
43. An S, Gao Y, Ling J, Wei X, Xiao Y. Calcium ions promote osteogenic differentiation and mineralization of human dental pulp cells: implications for pulp capping materials. J Mater Science: Mater Med. 2012;23(3):789–95.
44. Viti F, Landini M, Mezzelani A, Petecchia L, Milanesi L, Scaglione S. Osteogenic differentiation of MSC through calcium signaling activation: transcriptomics and functional analysis. PLoS ONE. 2016;11(2):e0148173.
45. He L, Zhang X, Liu B, Tian Y, Ma W. Effect of magnesium ion on human osteoblast activity. Braz J Med Biol Res. 2016;49(7):1–6.
46. Guarino V, Caputo T, Altobelli R, Ambrosio L. Degradation properties and metabolic activity of alginate and chitosan polyelectrolytes for drug delivery and tissue engineering applications. AIMS Mater Sci. 2015;2(4):497–502.
47. Pereira RF, Carvalho A, Gil M, Mendes A, Bártolo PJ. Influence of Aloe vera on water absorption and enzymatic in vitro degradation of alginate hydrogel films. Carbohydr Polym. 2013;98(1):311–20.
48. Wong YY, Yuan S, Choong C. Degradation of PEG and non-PEG alginate–chitosan microcapsules in different pH environments. Polym Degrad Stab. 2011;96(12):2189–97.

49. Domazetovic V, Marcucci G, Iantomasi T, Brandi ML, Vincenzini MT. Oxidative stress in bone remodeling: role of antioxidants. Clin Cases Mineral Bone Metabolism. 2017;14(2):209–16.
50. Das A, El Masry S, Gnyawali M, Ghatak SC, Singh S, Stewart K, Lewis R, Saha M, Gordillo A, Khanna G. S: Skin transcriptome of middle-aged women supplemented with natural herbo-mineral shilajit shows induction of microvascular and extracellular matrix mechanisms. J Am Coll Nutr. 2019;38(6):526–36.
51. Su P, Tian Y, Yang C, Ma X, Wang X, Pei J, Qian A. Mesenchymal stem cell migration during bone formation and bone diseases therapy. Int J Mol Sci. 2018;19(8):1–18.

Figures

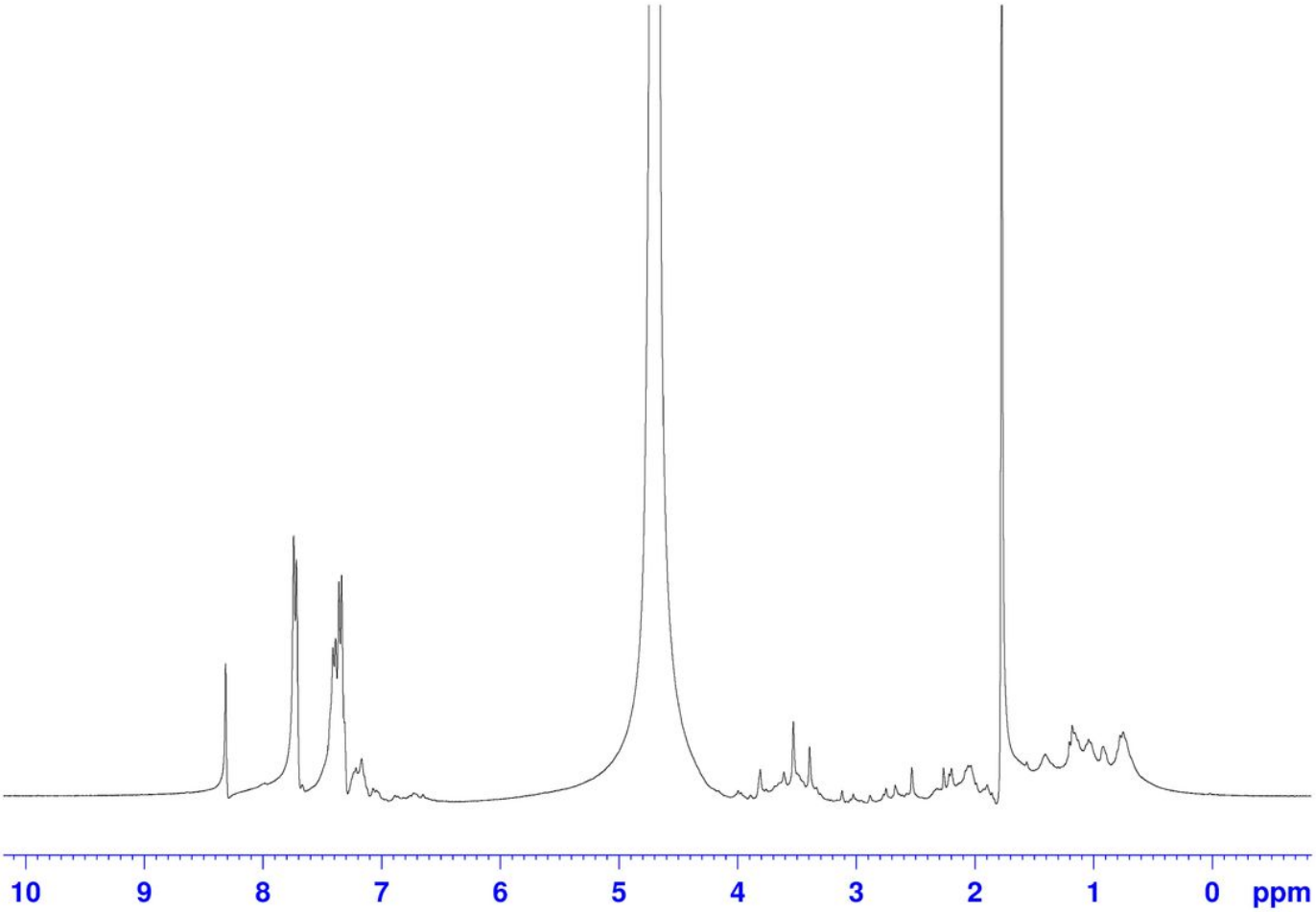

Figure 1

H NMR spectrum of Shilajit.

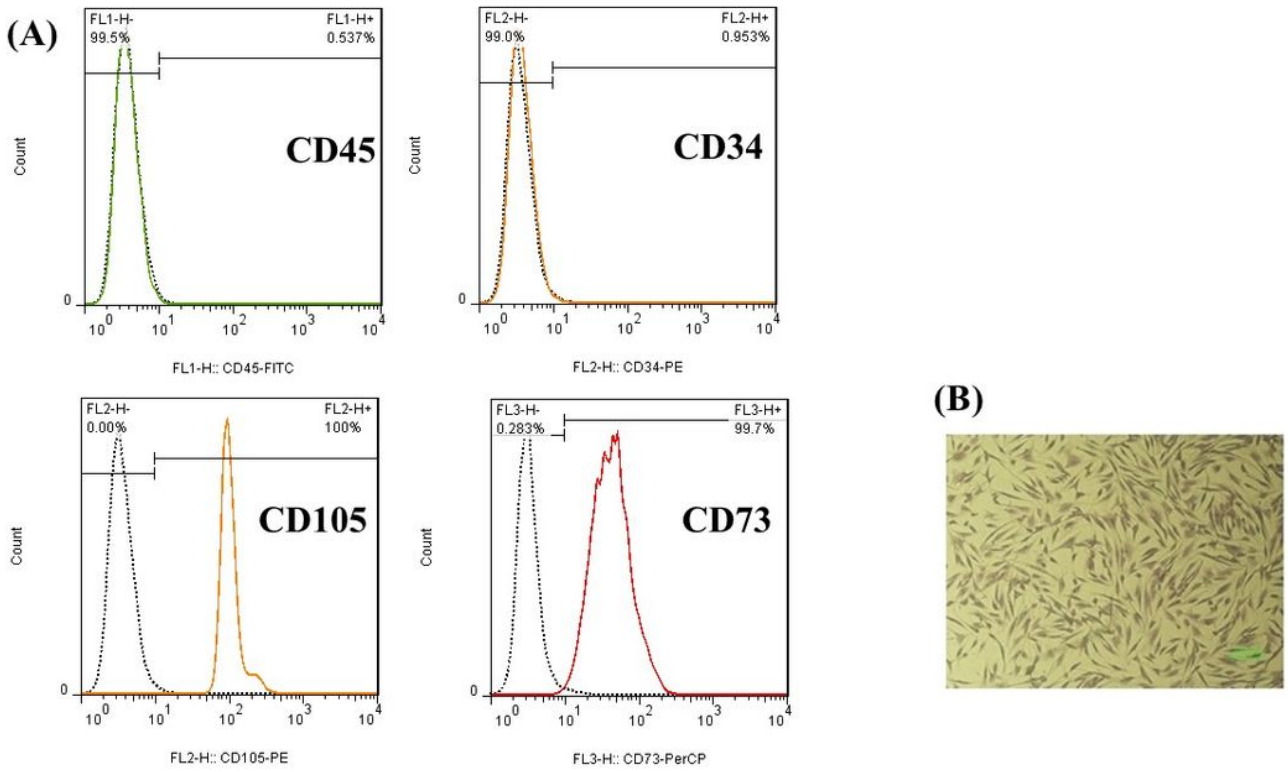

Figure 2

MSC characterization. (A) Flow cytometry indicated that ASCs were negative for CD45 andCD34 but positive for CD105 and CD73. **(B)** Isolated ASCs showed fibroblast-like shapes.

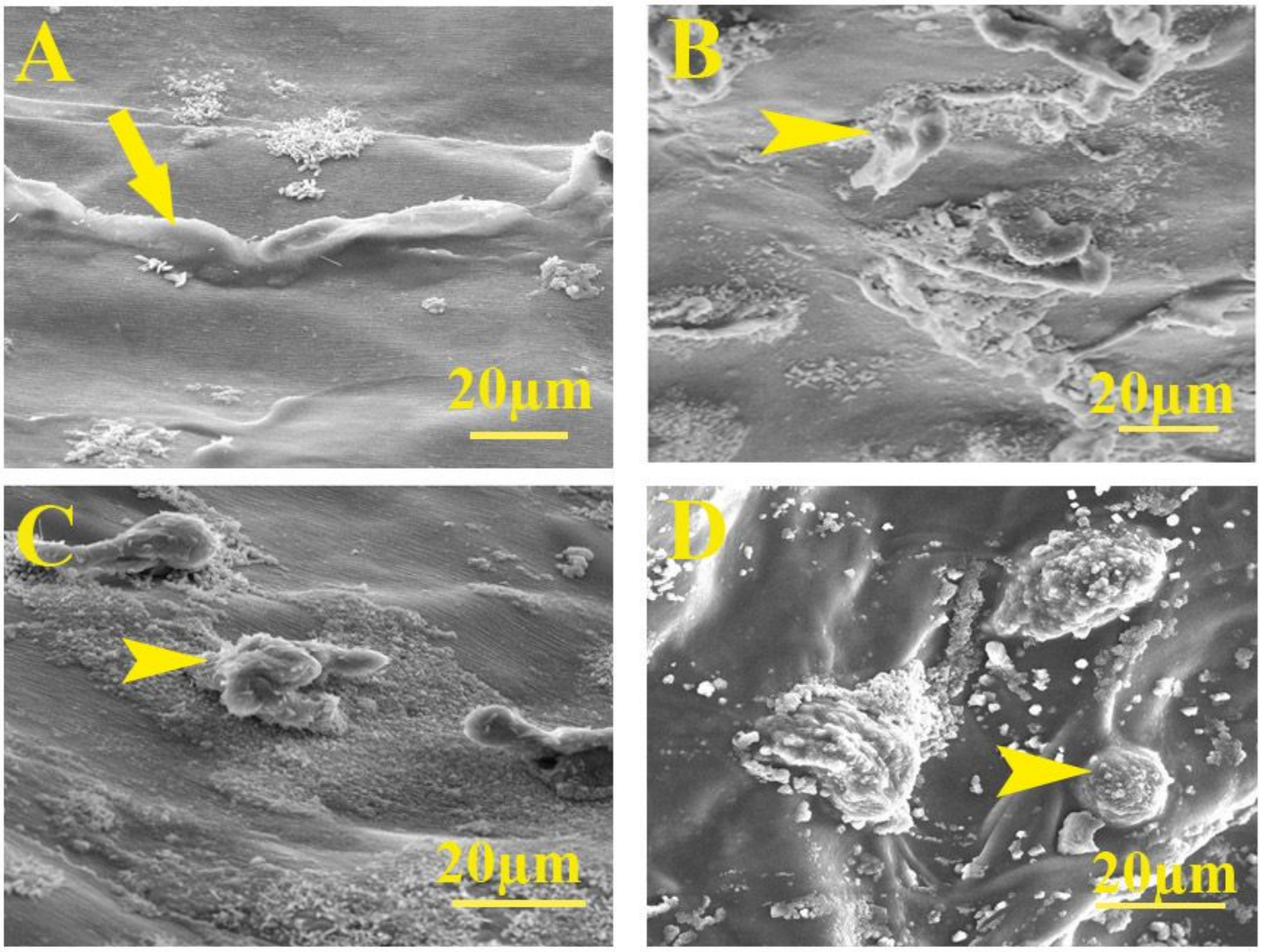

Figure 3

Scanning electron micrographs. **(A)** Cells with mesenchymal stem cell phenotype expanded in Alg/ASCs. Osteoblast-like cells with short processes on (**B)** Shilajit/Alg/ASCs+OM, **(C)** Shilajit/Alg/ASCs, and **(D)** Alg/ASCs+OM conditions.

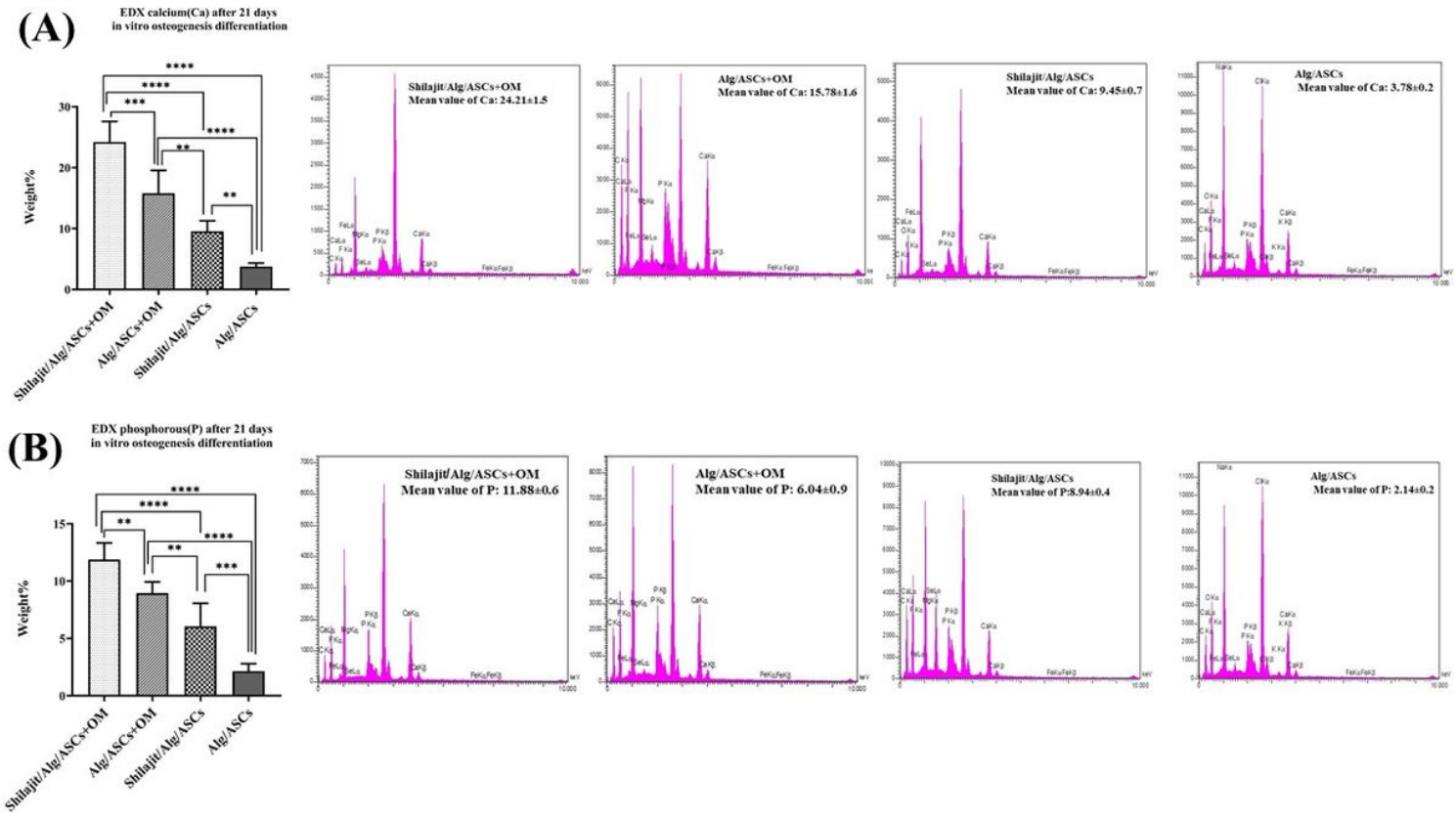

Figure 4

Energy Dispersive X-Ray Spectroscopy Analysis. Calcium (Ca, **A)** and phosphorus (P, **B)** contents in 3D groups after 21 days. The highest level of Ca and P was observed on Shilajit/Alg/ASCs+OM. The strongest peaks of Ca and P were shown on Shilajit/Alg/ASCs+OM (**P < 0.01, ***P < 0.001, ****P < 0.0001).

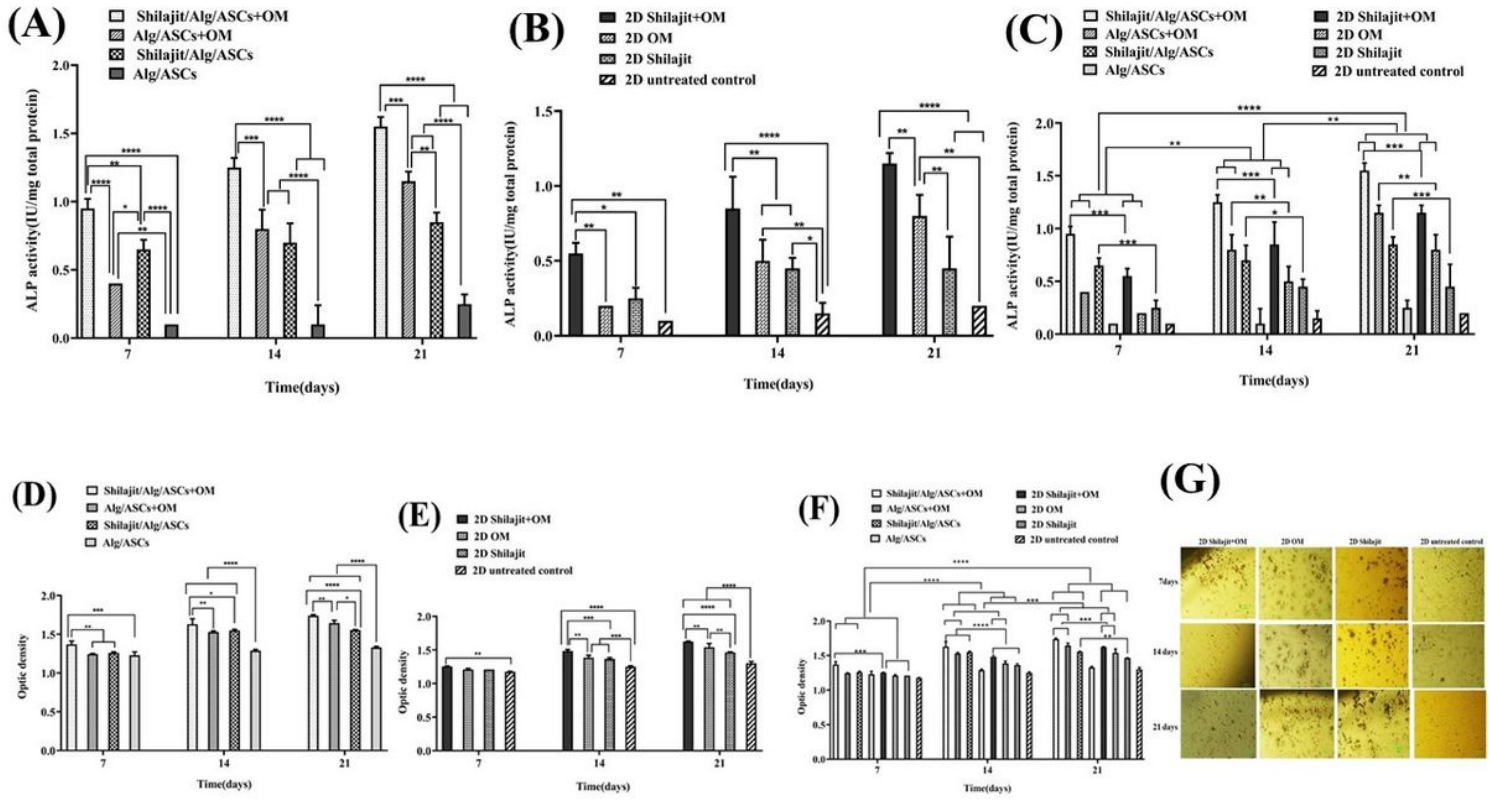

Figure 5

Mineralization assessments. The ALP activity (A, B, and C) and Calcium deposition (D, E, and F) assessments on different days of differentiation in 3D and 2D groups. G. Micrographs of cells stained with Alizarin red demonstrate the effects of shilajit on mineral deposition and nodule formation in 2D groups on 7, 14 and 21 days after differentiation. Qualitative observations showed that the number and size of the nodules increased in the presence of Shilajit (*P < 0.05, **P < 0.01, ***P < 0.001, ****P < 0.0001).

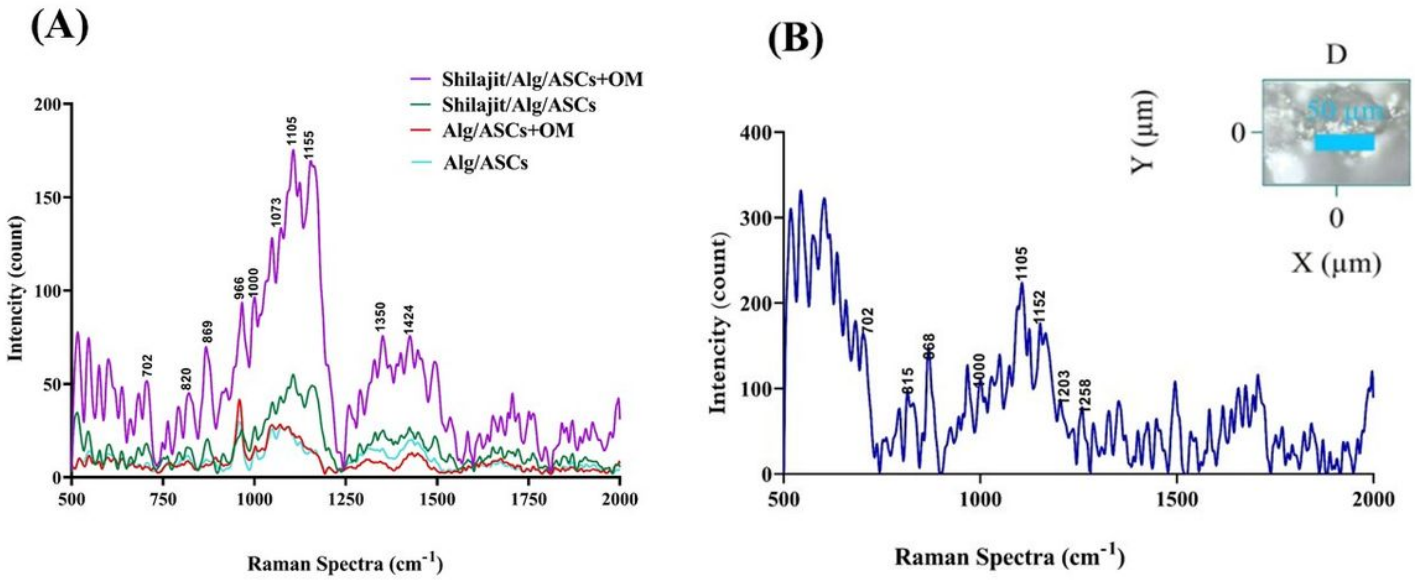

Figure 6

Raman confocal microscopy. (A) Raman spectra from 3D groups 21 days after differentiation show the peaks assigned for mineral and organic compounds related osteogenesis **(B)** Raman spectra profile for Shilajit.

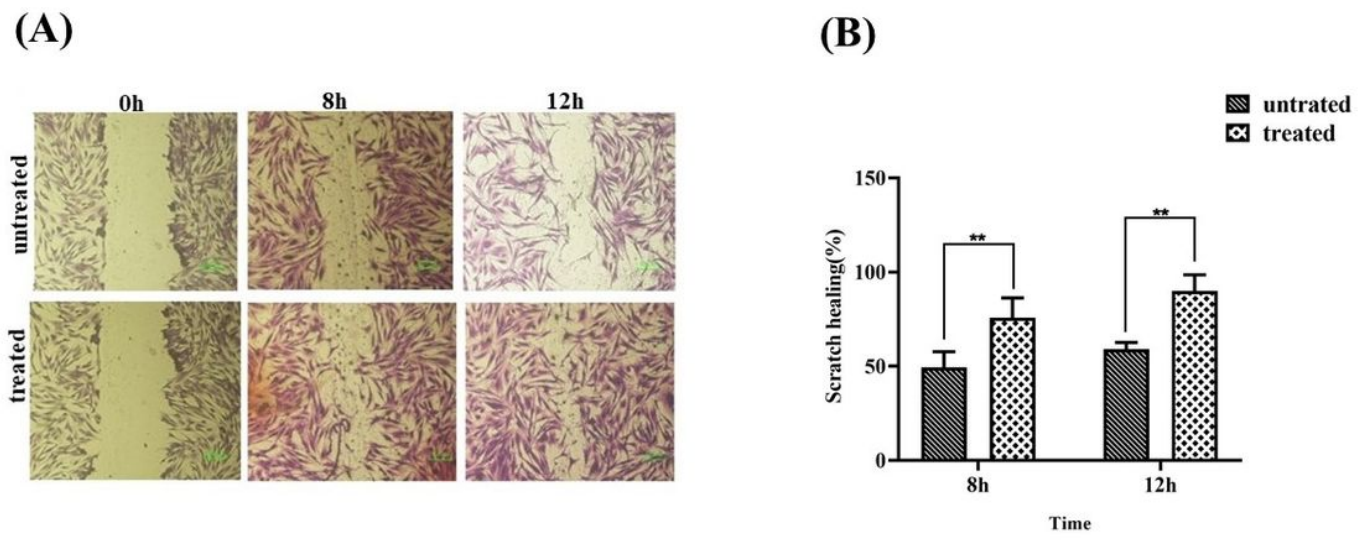

Figure 7

The effect of Shilajit on ASCs proliferation/movement rate in Shilajit treated and untreated groups. **(A)** Images were recorded at 0, 8 and 12 hours post-incubation (scale bar: 100 μm). **(B)** Healing/wounded area ratio in scratch healing analysis at 8 and 12 hrs.

** shows P<0.01.

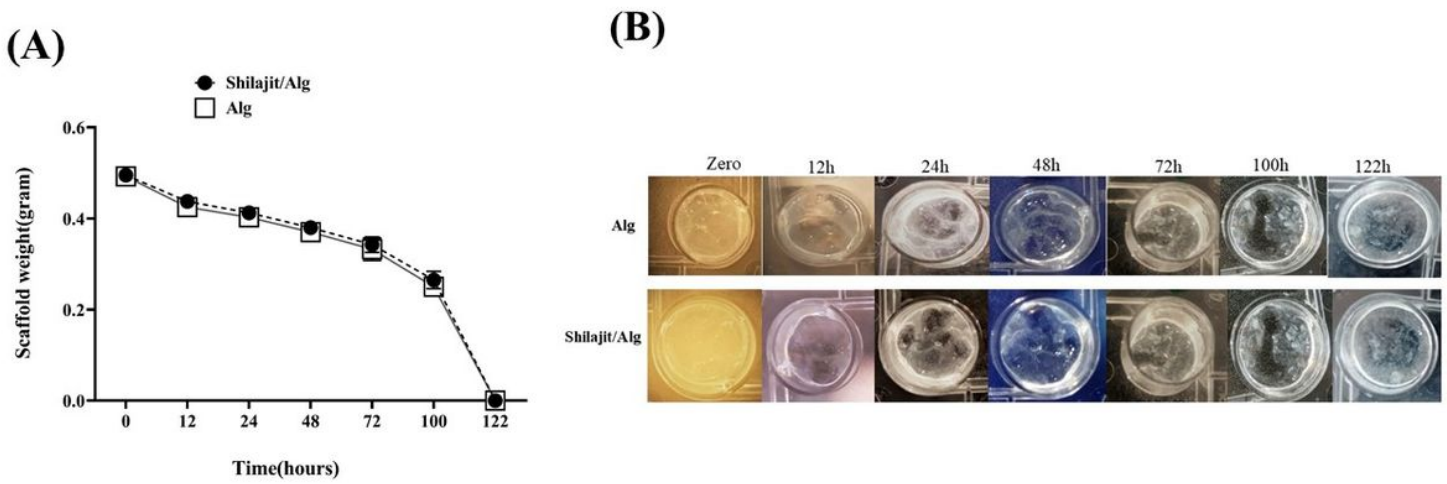

Figure 8

Image**(A)** and graph **(B)** show the same degradation rate in the scaffolds prepared with or without Shilajit.